Multiple possibilities for future precipitation changes in Asia under the Paris Agreement

Citation for published version:
Zhang, J, Wang, F, Tokarska, KB & Yang, Z 2020, 'Multiple possibilities for future precipitation changes in Asia under the Paris Agreement', *International Journal of Climatology*. https://doi.org/10.1002/joc.6495

Digital Object Identifier (DOI):
10.1002/joc.6495

Published In:
International Journal of Climatology

Multiple possibilities for future precipitation changes in Asia under the Paris Agreement

Jintao Zhang[a,b,#], Fang Wang[a*,#], Katarzyna B Tokarska[c], Zongliang Yang[d]

[a] Key Laboratory of Land Surface Pattern and Simulation, Institute of Geographic Sciences and Natural Resources Research, Chinese Academy of Sciences, Beijing, China; [b] College of Resources and Environment, University of Chinese Academy of Sciences, Beijing, China; [c] School of GeoSciences, University of Edinburgh, UK; [d] Jackson School of Geosciences, University of Texas at Austin, USA

* Correspondence: wangf@igsnrr.ac.cn; Tel.: +86-010-64889829

# J.Z. and F W. are the co-first authors, and they contributed equally to this work

Abstract

Future precipitation changes impact the availability of water resources and related flood and drought events. Recent studies have primarily focused on precipitation changes based on the Representative Concentration Pathways scenarios, which do not reflect the current mitigation commitments negotiated by governments under the Paris Agreement that aims to stabilize the global mean temperature at well below the 2.0°C threshold. Here, we analyze the Asian precipitation response to emission scenarios under warming resulting from the Intended Nationally Determined Contributions (INDC) pledges (as of August 2018), which would satisfy the Paris Agreement target in the next few decades. Our results show an increase in the mean precipitation in Asia by the end of this century by 12.9% (11.7%–14.7%) for a delayed action (No-policy) scenario, an increase by 8.0% (6.7%–8.8%) for a continued mitigation action (continued INDC-pledge) scenario, and an increase by 2.4% (1.9%–3.5%) and 4.4% (3.7%–5.4%) for scenarios that stabilize the global mean temperature at the 1.5°C and 2.0°C levels, respectively. However, spatial heterogeneity of precipitation changes reflects the complexity of precipitation responses in future climate projections. Furthermore, heavy rainfall events will strengthen with the enhanced warming, but the trend of dry spell events increases or decreases in different regions. Considering the impacts of precipitation-related extremes, we find that the projected population exposure to heavy rainfall and dry spell events will significantly increase in most Asian regions. Limiting warming to lower levels (such as 1.5°C or 2.0°C) would reduce the population exposure to heavy rainfall, thereby avoiding impacts associated with more intense precipitation extremes. These results contribute to an improved understanding of future risk from climate extremes, which is paramount for mitigation and adaptation activities for Asia, that is home of nearly 60% of the global population.

Key Words: INDC pledge; Precipitation; Extreme events; Dry spells; Extreme precipitation exposure;

1 Introduction

Global water cycle patterns are expected to change in a warmer world (IPCC, 2014). However, projected future changes in the water cycle are far more complex than projected temperature changes, including prominent regional and seasonal differences in the water cycle response to climate change (Collins et al., 2013). Some regions will be subject to decreasing hydrological activity whereas others may experience the opposite. Precipitation directly affects water resources for human survival, and precipitation-related extremes are among the most impact-relevant consequences of a warmer climate. Therefore, a more accurate projection of future precipitation changes, including the mean state and its extremes, is crucial for regions that heavily depend on hydrological cycle impacts on agriculture.

The Paris Agreement set a goal to restrict the global mean warming to well below 2.0°C above the pre-industrial level, and pursue efforts to limit the warming to 1.5°C (UNFCCC, 2015a, 2015b). To achieve this goal, countries submitted national mitigation plans in the form of Intended Nationally Determined Contributions (INDC). As of August 2018, a total of 192 countries have reported their respective INDC mitigation targets to the United Nations. The bottom-up approach of using national efforts reflecting the willingness of each country to reduce their emissions is easier to implement due to avoidance of different countries diverging from the distribution quota (Gupta et al., 2007).

Future emissions will be the key determinant of climate impacts in the next few decades. Recently, there are increasing efforts investigating changes in extreme climate events at the 1.5°C and 2.0°C warming levels, and the benefits of limiting global warming to 1.5°C rather than to 2.0°C (Donnelly et al., 2017; Dosio & Fischer Erich, 2017; Karmalkar & Bradley, 2017; King et al., 2018; King et al., 2017; Li et al., 2018; Schleussner et al., 2016; Sonia I. Seneviratne et al., 2018; Shi et al., 2018; Xu et al., 2017; W. Zhang et al., 2018; Hoegh-Guldberg et al., 2018; Zhou et al., 2018). However, these studies proposed idealized emission pathways for reaching the 1.5°C and 2.0°C global warming targets (Sanderson et al. 2016; Rogelj J 2016; UNEP 2017). Only a few recent studies make use of the INDC scenarios, but focus primarily on the global mean temperature responses (Fawcett et al., 2015; Rogelj et al., 2016; Sanderson et al., 2016; UNEP, 2017). Few studies evaluated the possible changes in regional precipitation and its extremes under the INDC emission pledges. Therefore, the socioeconomic system risks associated with precipitation change in the future are still unknown. Asia is the most populous continent in the world, and a variety of precipitation changes may affect different regions of Asia because of the diverse climate types. Regional assessments of flood and/or drought risks and the impacts that could be avoided by limiting warming to a low level are critical for mitigation and adaptation planning.

Here, we examine the response of Asian precipitation to emission reductions from the INDC under the Paris Agreement for the next few decades, using an ensemble of comprehensive Earth System Models (ESM) from the Fifth Coupled Climate Model Intercomparison Project (CMIP5). Considering the socioeconomic impacts of future climate change, we further explore the risk of precipitation-related extremes under the INDC emission scenario.

2 Data and Methods

2.1 Emission scenarios

We analyzed the INDC emissions data submitted by 192 countries according to the Paris Agreement. The INDC reports are continuously updated and include 165 INDCs that submitted their pledges through 2018 (Oct.), in which the member states of the European Union (EU) submitted one INDC target for the whole region. The INDC reports from each country were obtained from the UNFCCC website (UNFCCC, 2018). National INDC commitments provide emission targets for the pre-2030 period. The reported emission targets of countries vary from absolute to relative to a base year level, or emission reduction targets relative to a baseline emission scenario. We analyzed and extracted the emission targets of most countries. For more detailed information about the INDC dataset, refer to Supplementary Material S1 and Table S1.

In order to extend the INDC emission scenarios to the end of the 21st century, simulations of future emissions from 28 socioeconomic models were used (Table S2). We considered the rate of decarbonization, carbon capture and storage technology (CCS), energy structure improvement, time to carbon neutralization, etc. Here, we consider many possible interpretations of "INDC mitigation actions" as available in the scenarios that contributed to the IPCC AR5 Scenario Database. We use scenarios that conform to 2030 greenhouse gases (GHG) emission levels consistent with the INDCs (50–56 $GtCO_2eq/yr$) and assume no sudden changes in climate action over the 21st century. Considering the difficulty and uncertainty of carbon removal technology in the future, we take a conservative approach regarding the future availability of negative emissions technologies and scenarios with CCS > 15 Gt CO_2eq/yr are eliminated. A total of 67 pathways meet the criteria, which are shown in Fig. 1.

The derived emission scenarios were then classified into six groups based on some key characteristics (e.g. emission targets for specific years, renewable energy structure, and the amount of CCS), as shown in Fig. 1. Group I (baseline scenario) contains scenarios without any additional climate policies nor mitigation actions, where the GHG emissions continue to grow according to current trends. Group II is similar to the baseline scenario but allows for lower energy intensity in the future. Group III represents a weak-policy baseline scenario considering existing climate policies, a weak interpretation (e.g., 2020 Copenhagen Pledges), and extrapolation of these targets beyond 2020 based on emissions intensity. Global emissions were assumed to peak in 2030 in Groups IV to VI. Specifically, Group IV can be described as a "continued action" pathway. The relatively constant decarbonization rates were roughly followed for the period after 2030. The overall trend of Group V is close to that of Group IV, but more rapid mitigation after 2030 is the distinguishing characteristic. Group VI involves CCS action accelerating decarbonization and determining negative emissions in some pathways.

In the discussion below, we refer to Groups I as the "delayed action" (No-policy) scenario, and Group IV as the extended "continued action" (INDC-pledge) scenarios (Tokarska et al., 2016; Wang et al., 2018). The patterns of climate responses at the 1.5°C and 2.0°C levels of warming are given to be compared with the INDC scenarios.

Figure 1. Future emission pathways analyzed in this study. The black vertical line represents the range of conditional and unconditional INDC pledges in 2030; thin lines in different colors show the selected emission pathways clustered into the six groups. The range of the 1.5°C and 2.0°C pathways are plotted for reference, in grey and orange shaded areas, respectively (CAT, 2017). The estimates of warming at the end of the 21st century above the pre-industrial level (ΔT) for each scenario group are labelled on the right (uncertainty range of 33-66% and median in brackets).

2.2 Estimation of climate response to INDC emissions

We first estimated the global warming levels under different INDC scenarios (Fig. 1) via the relationship between the transient climate response and cumulative CO_2 emissions in CMIP5 (Collins et al., 2013; Gillett et al., 2013; Matthews et al., 2009; Tokarska et al., 2016; Zickfeld et al., 2009). Cumulative emissions and corresponding temperature responses for all CMIP5 models are based on 78 simulations. A function of temperature change responses to cumulative CO_2 emissions ($TCRE_{all}$) was constructed from multimodel simulations, defined as: $TCRE_{all} = \frac{\Delta T}{\Delta I}$, where ΔI represents the cumulative anthropogenic CO_2 emissions and ΔT is the corresponding change in global mean temperature, subject to decadal smoothing. All non-CO_2 emissions in INDC scenarios were converted into a unit of CO_2 equivalent emissions. The warming in response to the INDC scenarios (ΔT_{INDC}) was calculated from the equation: $\Delta T_{INDC} = TCRE_{all} \times \Delta I_{INDC}$, where ΔI_{INDC} represents the cumulative emissions under the INDC scenarios. More details on this method can be found in Supplementary Material S4.

Furthermore, the regional climate change at INDC-induced warming levels were derived from the CMIP5 multimodels using the time-slice approach. Nineteen comprehensive ESMs from the CMIP5 archives were used (Taylor et al., 2011), which have different levels of climate sensitivity (Gillett et al., 2013), and represent a wide range of climate responses to emission scenarios (see Table S3). Historical simulations (1861–2005) and future projections of Representative Concentration Pathway 8.5 (RCP8.5) scenario (2006–2100) were adopted in this study. All model data was interpolated to a common 1.5°×1.5° horizontal grid. The spatial pattern of the climate was identified using a time-slice approach, where the spatial state at a specific warming point related to ΔT_{INDC} was taken from the decadal time slices with the respective mean warming for each model separately (Supplementary Material S4 and Fig. S1). The spatial simulations of future climate change are based on the multimodels ensemble. To indicate the significance of climate change, we assessed the signal to noise ratio (SNR), expressed as the significance of change compared to internal variability (Supplementary Material S4 and Figs. S2, S3, S4).The period of 1985–2005 is referred to as the present day baseline and the preindustrial period is defined as 1861–1900.

The changes in mean precipitation and its extremes in Asia were analyzed. Considering the spatial variation of climate response to global INDC emissions, Asia is classified into six sub-regions defined by Hijioka et al., (2014): East Asia (EA), Southeast Asia (SEA), South Asia (SA), West Asia (WA), North Asia (NA) and Central Asia (CA) (Fig. 2 and Supplementary Material S2).

Figure 2 Sub-regions in Asia.

2.3 Assessment of Risks from Extreme Events

Extreme precipitation events can be defined using either relative or absolute thresholds. Here, we employ the frequently used ETCCDI Climate Change Indices: the RX5day (Maximum accumulated 5-day precipitation) and CDD (Maximum dry spell length, defined as consecutive days with precipitation < 1 mm) (Seneviratne et al., 2012; Zhang et al., 2011). CDD is only an indicator for dry spell length and does not account for changes in evapotranspiration and soil-moisture related effects. Therefore, it should not be interpreted as a direct indicator of agricultural or hydrological drought (Mueller & Seneviratne, 2012; Orlowsky & Seneviratne, 2012). Nevertheless, CDD and the RX5day can be seen as proxies for the precipitation component when assessing drought and flood risks, respectively. The results and impacted regions identified here are broadly consistent with projections based on more comprehensive indicators for droughts (Dai, 2012; Prudhomme et al., 2014) and flood risk (Hirabayashi et al., 2013).

Regarding social impacts, extreme events that deviate substantially from their climatology can result in the greatest losses. The response of extreme precipitation to global warming is twofold and depends on its mean state and variability. Increases in precipitation mean and/or variability would increase the frequency of intense extreme events that could be dangerous in terms of social impacts (Viatcheslav V. Kharin & Zwiers, 2005). Climate change risks are typically determined by the hazards, vulnerability, and exposure of human society and natural ecosystems (Lavell et al., 2012). Climate extreme indices (Rx5day and CDD) characterize the intensity of hazards. For further analysis, we define dangerous extreme events as those exceeding specific return values (RVs) from the 1961–2005 baseline (V. V. Kharin et al., 2018), and quantify the changes in exposure to hazards (extreme precipitation and dry spells) under different scenarios. Technical details on the calculation of exposure are described in Supplementary Material S5. This article does not discuss the vulnerability of social-economical systems, and the results of exposure reflect only the risk of physical climate change.

Extreme precipitation and dry spells response to the global INDC scenarios were calculated based on the CMIP5 models. Furthermore, we investigated the avoided impacts at different warming levels that correspond to different mitigation policies. We quantify those impacts as the difference in exposure between a given warming level k and the present-day baseline (1985–2005), expressed as a ratio:

$$\text{impacts}\ \ (\mathrm{k}) = \frac{E_k - E_{present}}{E_{present}} \times 100\% \tag{1}$$

where E stands for the exposure and the subscript k indicates different warming levels from different scenarios (1.5°C, 2.0°C, INDC-pledge, No-policy; as in Fig. 1). Thus, the impacts avoided by limiting warming from warming level k_1 to a lower level k_2 are expressed as the diffenences between $\text{impacts}\ \ (k_2)$ and $\text{impacts}\ \ (k_1)$.

3 Results

3.1 Changes in mean precipitation

Figure 3. Relative changes in annual mean precipitation over Asia, absed on multi-model median. Colored shading is applied for areas where at least 66% of the models agree on the sign of the change; black stippling indicates regions where at least 90% of all models agree on the sign of the change.

Figure 4. Regional average differences among different scenarios in the annual mean precipitation changes in Asia and the six sub-regions. Central lines and bars in blue denote multimodal medians and interquartile ranges, respectively. Horizontal dashed and solid lines in grey indicate the value of Asian mean and zero, respectively.

The changes in annual mean precipitation over Asia and the six sub-regions (Supplementary Material S2) until the end of the century exhibit contrasting patterns in terms of signal strength and robustness (Fig. 3). Uncertainty in model precipitation projections is considerably larger than that for temperature (Collins et al., 2013). Regional averages and the relative differences between the various sets of scenarios are also shown in Fig. 3 for each subregion. Precipitation over Asia will increase by 2.4% (1.9%–3.5%; range of the 25%–75% confidence interval, and the same confidence interval applies to subsequent values) in the 1.5°C scenario, 4.4% (3.7%–4.4%) for the 2.0°C scenario, 8.0% (6.7%–8.8%) for the INDC-pledge scenario, and 12.9% (11.7%–14.7%) for the No-policy scenario, compared to the present day baseline. Furthermore, under the INDC-pledge scenario, there is a greater increase in precipitation in NA (12.4%), followed by CA (7.0%), EA (6.2%), SA (5.8%), and SEA (4.5%), but precipitation decreases in WA (-3.6%). Under the No-policy scenario, the projected precipitation increases are in the following regions: NA (20.5%), WA (12.3%), EA (11.15%), SA (9.0%), SEA (7.7%), and CA (6.5%). There is increasing uncertainty in the projected changes under the No-policy scenario, since fewer models would reach such a high warming under the simulation of RCP8.5 (Fig. S1). Considering the differences between the two future scenarios, there are less significant changes in precipitation between the 1.5°C and 2.0°C scenarios (2.0°C versus 1.5°C), compared with that beween the 2.0°C and INDC scenarios (INDC versus 2.0°C), in Asia as a whole and in most of its sub-regions (Fig. 4). Changes with high agreement among models appear mainly in NA and northern EA, but the sign of regional mean precipitation change can be positive or negative in WA, CA, SEA, and SA, reflecting water cycle projection uncertainty (Fig. 3).

With an increase in the warming levels, overall precipitation in Asia also increases but has a different regional characteristics. Most significant increases are found mainly in NA, whereas there is a little decrease in WA (and some in borderlands of CA and SA) where the intermodel range is the largest (Fig. 3).

Figure 5. **Annual mean precipitation response to global temperature increase, per degree of warming.** Regression coefficients are calculated in each grid cell based on the local precipitation and global mean temperature of seperate models, and then adopted the multimodel ensemble median. **Left**: Spatial distribution of multimodel median: colored shading is applied for areas where at least 66% of the models agree on the significant linear relationship (statistically significant at the 5% level based on the Student's t-test); black stippling indicates regions where at least 90% of all models agree on the significant linear relationship.. **Right**: Regional average: Central lines and bars show the multimodel ensemble 25th, 50th, and 75th intervals.

We further examined the relationship between precipitation changes and global warming (Figs. 5 and S5). The mean precipitation averaged over Asia responds approximately linearly with the global mean temperature increase at a rate of 4.4% K^{-1}, with a 25th–75th percentile range of 1.6–6.6% K^{-1} (Fig. 5), but the regression coefficient varies greatly among regions. The most prominent response occurs in NA (6.0% K^{-1}). The regression coefficients are close to zero in CA (0.9% K^{-1}) and WA (-0.7% K^{-1}); this indicates that the change in mean precipitation in those regions with global warming is not significant. In addition, coefficients in EA (4.0% K^{-1}), SEA (2.8% K^{-1}), and SA (3.0% K^{-1}) are lower than the mean state of the whole continent.In most regions, such a response is lower than that expected from the Clapeyron–Clausius equation (an increase rate of about 7% K^{-1} of atmospheric moisture). The weaker response of the mean precipitation can be partly explained by the energy constraints (Allen and Ingram 2002; Held and Soden 2006).

3.2 Changes in precipitation extremes

Figure 6. **Relative changes in the annual Rx5day over Asia, based on the multi-model median.** Increased dryness is indicated with yellow to orange colors; decreased dryness with blue. Colored shading is applied to areas where at least 66% of the models agree on the sign of the change; stippling is added for regions where at least 90% of all models agree on the sign of the change.

Figure 7. **Relative change in annual CDD over Asia, based on the multi-model median.** Corresponds to Fig. 6, but for CDD.

Considering changes in the precipitation extremes, we use the Rx5day (Maximum accumulated 5-day precipitation) for characterizing heavy rainfall events and CDD (the maximum dry spell length, defined as consecutive days with precipitation < 1 mm) for long dry spell events. Figs. 6 & 7 show the median estimates for projected RX5day and CDD indices, respectively. We first focus on the changes in the Rx5day index in the 1.5°C, 2.0°C, INDC-pledge, and No-policy scenarios. There is a consistent increasing extreme precipitation trend under global warming in Asia, but the magnitudes of those changes are widespread across the different sub-regions (Fig. 6). The regions with profound increases in extreme precipitation include Siberia, the Tibetan Plateau and its surroundings, the Indian subcontinent and Indonesia. In contrast to the uniform change in the Rx5day, the changing CDD signs show regional differences (Fig. 7). CDD in the high latitude in NA shows a significant decreased trend, but there is an increasing trend in most areas of EA, SEA, and the edge of the Tibetan Plateau. The CDD model uncertainty is remarkably greater than the Rx5day, and WA and western SA are areas of high uncertainty in both the Rx5day and CDD. In addition, there are large differences in the projected CDD in CA region among the models.

3.3 Changes in exposure to precipitation-related extremes

Figure 8. **Population exposure to heavy rainfall events of different RVs.** The population density weighted means for Asia and the six sub-regions are estimated based on the year-2100 population projection under the SSP2 scenario (for future scenarios) and the year 2000 baseline (for present day). The multimodel medians are in solid lines, and interquartile ranges are shaded. Results of areal exposure refer to Fig. S6.

Figure 9. **Population exposure to dry spell events of different RVs.** Corresponds to Fig. 8, but for population exposure to dry spell events. Results of areal exposure refer to Fig. S7.

To further analyze the impact of precipitation-related extremes, we define dangerous extreme events as those exceeding the 10-, 20- and 50-year RVs from the present day baseline (1961–2005), and lie in the upper tail of the extreme value distributions. The three thresholds represent different levels of danger. Exposures to extreme events exceeding those RVs under different scenarios are estimated, and then the population density weighted regional average exposure is computed (Supplementary Material S5). Here, we only show the population exposure estimated from the projected population in the year 2100 under the SSP2 scenario (Jones & O'Neill, 2016), whereas the population exposures based on projections under other SSP scenarios are qualitatively similar. The evolution of exposure (especially population density weighted exposure) with warming levels indicates the probability of the human system being impacted by these dangerous extremes. Asia and its sub-regions exposed to these dangerous events increases consistently with global warming, and record-breaking events will be more frequent in the future.

Considering the whole Asian average, for heavy rainfall events that exceed the baseline 20-year RV, the population exposure increases from the present-day level of 6.0% (5.9%–6.5%) to 8.1% (7.2%–10.2%) for the 1.5°C scenario, 9.5% (8.3%–11.9%) for the 2.0°C scenario, 14.8% (10.0%–16.4%) for INDC-pledge scenario, and 18.9% (14.6%-21.5%) for the No-policy scenario (Fig. 8). Similarly, the population exposure to long dry spell events that exceed the baseline 20-year RV increases from 5.3% (4.6%–6.1%) for the present day to 6.5% (4.7%–8.5%) for the 1.5°C scenario, 6.9%

(5.0%–8.4%) for the 2.0°C scenario, 6.3% (4.5%–10.2%) for the INDC-pledge scenario, and 7.7% (5.0%–12.7%) for the No-policy scenario (Fig. 9). The increased rate of exposure to heavy rainfall events with global warming is remarkably faster than that for dry spell events, and the greater uncertainty of projected CDD results in a larger intermodal variable of exposure to dry spell events.

Compared with the results of population exposure and the Rx5day/CDD indices, the trends of change are similar in most sub-regions. Some inconsistent events, such as the NA region, with significant decrease in CDD facing a higher risk of dry spell than that in the present day, can be explained by the population distribution.

3.4 Avoided impacts in low warming scenarios

Figure 10. Changes in extreme heavy rainfall (two left panels) and dry spell events (two right panels) avoided over Asia and its sub-regions in less warming scenarios. Population exposure is reduced in the low warming scenarios (1.5°C compared to 2.0°C, 2.0°C compare to INDC pledge) for heavy rainfall (columns 1 and 2) and dry spell (columns 3 and 4) events that exceed the baseline (a) 10-, (b) 20- and (c) 50-year return values. Central lines and bars denote multimodal medians and interquartile ranges, respectively. Results based on areal exposure refer to Fig. S8.

If warming is limited to a lower level, the Asian region is projected to benefit from robust reductions in population exposure to dangerous extremes (Fig. 10). Over the whole Asian region, for heavy rainfall (Rx5day) events that exceed the baseline 20-year RV, population exposures over the present-day level will increase to 134% (122%–157%) for the 1.5°C scenario, 156% (141%–182%) for the 2.0°C scenario, 244% (170%–253%) for the INDC-pledge scenario, and 311% (248%–331%) for the No-policy scenario. Thus, the median values of avoided impacts are estimated to be 34% (18%–40%) (1.5°C versus 2.0°C) and 30% (18%–75%) (2.0°C versus INDC-pledge). In the same way for dry spell (CDD) events, the median values of avoided impacts are estimated to be 12% (-1%–18%) (1.5°C versus 2.0°C) and 15% (-5%–38%) (2.0°C versus INDC-pledge), respectively, for population exposures exceeding the baseline 20-year RV due to a lower warming level. It is worth noting that the avoided impacts are more remarkable for more intense extremes. For example, for the heavy rainfall events exceeding the baseline 50-year RV, the population exposures that could be reduced by less warming amount to 39% (29%–61%) (1.5°C versus 2.0°C) and 54% (31%–82%) (2.0°C versus INDC-pledge). More than half of the sub-regions would experience such robustly avoided impacts, although the magnitudes would differ. For the dry spell events exceeding the 50-yr RV, the avoided impacts amount to 24% (1%–34%) (1.5°C versus 2.0°C) and 37% (-14%–63%) (2.0°C versus INDC-pledge), respectively. However, uncertainty ranges of avoided impact for dry spell events stretch across zero for most sub-regions, indicate no statistical significant difference among scenarios.

In low warming scenarios, almost all regions in Asia will face less risk (exposure) of heavy precipitation and dry spell, and the reduced exposure to extreme heavy rainfall events due to lower warming is larger than for extreme dry spell events. Hotspots where the avoided impacts are the most prominent are seen in CA (for heavy rainfall events) and WA (for dry spell events). We only consider the fractional population exposure. If the absolute population growth is considered, the avoided impacts will be larger.

4 Discussion

Climate warming in response to the actual emission reductions stipulated by the Paris Agreement is receiving significant interest. Most of the existing research is based on RCP or 1.5°C and 2.0°C scenarios. However, these scenarios do not account for the current mitigation commitments negotiated by governments. Our approach is based on the self-determined emission reduction commitments reached in the climate negotiations as the starting point to assess climate response in the future.

We use simulations from the CMIP5 models to quantify regional climate changes in response to INDC pledges and their extensions. Our results indicate that climate warming under the INDC scenarios is projected to greatly exceed the long-term Paris Agreement goal of stabilizing the global mean temperature above the 2.0°C or 1.5°C levels. The differences in exposure to extreme events between different scenarios is found to be more than that of the mean state. Our results indicate that if global emission reductions are further strengthened to achieve ambitious temperature targets, such as the Paris Agreement goal, the benefits on regional heavy precipitation and dry spell risk may be more pronounced than on the mean state of precipitation. The impact-relevant extremes, changes in the water cycle, and particularly the availability of water on the uncertain warming in the future deserve further investigation (Sebastian et al., 2016).

Nearly all previous studies are based on existing CMIP5 data, which were not specifically designed for assessment. The National Center for Atmospheric Research (NCAR) released a set of climate simulations to assess the impacts of 1.5°C and 2.0°C warmer climates using the Community Earth System Model (CESM), which entail only stabilization pathways that reach 1.5°C and 2.0°C warming levels (B. M. Sanderson et al., 2017) and are not specific to the INDC pledges, which are the focus of this study. When analyzing the climate response to global INDC emissions, targeted experimental design is still lacking; thus, it is difficult to accurately estimate the equilibrium state of the climate response under a specific temperature rise threshold based on existing climate change projection results.

Our study uses the time-slice approach applied to the INDC pledges, using the fully coupled CMIP5 models, as opposed to the atmosphere-only coupled models used by Mitchell et al. (2017) and in the HAPPI experiments. The fully coupled runs could generate comprehensive extreme events than the atmosphere-only run (prescribed sea surface temperature). We focus not only on the assessment of extreme climate impacts under INDC scenarios, but also on the extreme climate impacts at 1.5°C. Our results under the 1.5°C scenario are consistent with those presented in Chapter III of the IPCC 1.5°C report (Hoegh-Guldberg et al., 2018). We further show that the risk of climate extremes and their impact on the regional socioeconomic systems considered here will be significantly different under various scenarios that entail emissions from the INDC, and the 1.5°C warming target. We show that less warming lowers the risk of extreme events in the Asian regions.

We also recoginze that the TCRE framework used in this study was primarily designed for CO_2-only emissions. Converting INDC emissions to CO_2-equivalent emissions does not account for different life-time of different forcers (such as short-term but high warming impact from the methane emisisons). Newer approaches suggesting a forcing-equivalent (rather than CO_2-emissions equivalent) metric (Allen et al., 2018) would be more suitable, but cannot be easily computed from the data available in the CMIP5 archive.

The large-scale ESMs continue to show less consistent changes for precipitation than for surface temperature. It is worth noting that the uncertainty ranges of the projected precipitation seem to be large. On one hand, it is challenging to simulate the physical process related to precipitation accurately in existing ESMs. On the other hand, the intermodal dispersion is not simply equal to uncertainty. For example, every model has its own design and parameterizations of key processes, and every model and its output was assumed to be equally valid, even though some models perform better than others in certain ways when tested against historical records.

5 Conclusion

Using fully coupled simulations from 19 CMIP5 models, we analyze changes in precipitation and its extremes over Asia under global INDC scenarios, and compare the results at the 1.5°C and 2.0°C warming thresholds. The differences in Asian climate change in response to different emission scenarios substantially differ at a regional scale. The main findings are summarized as follows:

(1) The mean precipitation averaged over Asia is expected to increase by 2.4% (1.9%–3.5%) under the 1.5°C scenario, 4.4% (3.7%–4.4%) for the 2.0°C scenario, 8.0% (6.7%–8.8%) for the INDC-pledge scenario, and 12.9% (11.7%–14.7%) for the No-policy scenario, relative to the present-day level. In general, concurrent with enhancement of global warming, there will be a gradual increase in precipitation, generally with a larger response in high latitudes than in mid-low latitudes. The inter-model range is large in WA, CA, and western SA regions, indicating the uncertainty in precipitation projection. The change in mean precipitation response to global mean warming is lower than that expected from the Clapeyron–Clausius equation and the appearance of regional features.

(2) With the strengthening of global mean warming, the intensity of heavy rainfall events over Asia will substantially increase, indicating more frequent extreme heavy rainfall. However, the change in dry spell events shows complex regional characteristics, with greater differences between models. There dry spells will be shorter in high latitudes but longer in some monsoon regions.

(3) The population exposure to dangerous extreme precipitation events (e.g. exceeding the 20-year RV) is expected to increase consistently with warming over Asia, and there is a higher risk of record-breaking heavy precipitation events than dry spell events in the future. Less warming would reduce population exposures to once-in-20-year extreme heavy rainfall events over Asia by 34% (18%–40%) (1.5°C versus 2.0°C) and 30% (18%–75%) (2.0°C versus INDC-pledge). For extreme dry spell events, the reduced exposures over Asia are estimated to be 12% (-1%–18%) (1.5°C versus 2.0°C) and 13% (-5%–38%) (2.0°C versus INDC-pledge). The avoided impacts in lower warming scenarios are more significant for the intense extremes. However, the projected exposure to dry spell events remain larger uncertainties, and there are no significant differences among scenarios in most sub-regions. These results provide a better understanding of the future risk associated with climate extremes, which is essential for mitigation and adaptation activities for Asia, that is home to nearly 60% of the global population (Center for International Earth Science Information Network et al. 2005).

References

Allen, M. R., & Ingram, W. J. Constraints on future changes in climate and the hydrologic cycle. Nature, 2002, 419 (6903), 224.

Allen, M. R., Shine, K. P., Fuglestvedt, J. S., Millar, R. J., Cain, M., Frame, D. J., & Macey, A. H. (2018). A solution to the misrepresentations of CO2-equivalent emissions of short-lived climate pollutants under ambitious mitigation. *npj Climate and Atmospheric Science,* 1(1), 16. https://doi.org/10.1038/s41612-018-0026-8.

CAT. (2017). Addressing global warming. Retrieved from https://climateactiontracker.org/global/temperatures/.

Center for International Earth Science Information Network—CIESIN—Columbia University, United Nations Food and Agriculture Programme—FAO, and Centro Internacional de Agricultura Tropical—CIAT. Gridded Population of the World, Version 3 (GPWv3): Population Count Grid. (NASA Socioeconomic Data and Applications Center (SEDAC): Palisades, NY, 2005). https://doi.org/10.7927/H4639MPP. Accessed 3rd November 2019.

Collins, M., Knutti, R., Arblaster, J., Dufresne, J.-L., Fichefet, T., Friedlingstein, P., et al. (2013). Long-term Climate Change: Projections, Commitments and Irreversibility. In T. F. Stocker, D. Qin, G.-K. Plattner, M. Tignor, S. K. Allen, J. Boschung, A. Nauels, Y. Xia, V. Bex, & P. M. Midgley (Eds.), *Climate Change 2013: The Physical Science Basis. Contribution of Working Group I to the Fifth Assessment Report of the Intergovernmental Panel on Climate Change*. Cambridge, UK, and New York, NY, USA: Cambridge University Press.

Dai, A. (2012). Increasing drought under global warming in observations and models. *Nature Climate Change, 3*, 52. http://dx.doi.org/10.1038/nclimate1633.

Donnelly, C., Greuell, W., Andersson, J., Gerten, D., Pisacane, G., Roudier, P., & Ludwig, F. (2017). Impacts of climate change on European hydrology at 1.5, 2 and 3 degrees mean global warming above preindustrial level. *Climatic Change, 143*(1), 13-26. https://doi.org/10.1007/s10584-017-1971-7.

Dosio, A., & Fischer Erich, M. (2017). Will Half a Degree Make a Difference? Robust Projections of Indices of Mean and Extreme Climate in Europe Under 1.5°C, 2.0°C, and 3°C Global Warming. *Geophysical Research Letters, 45*(2), 935-944. https://doi.org/10.1002/2017GL076222.

Fawcett, A. A., Iyer, G. C., Clarke, L. E., Edmonds, J. A., Hultman, N. E., McJeon, H. C., et al. (2015). CLIMATE POLICY. Can Paris pledges avert severe climate change? *Science (New York),* 350(6265), 1168-1169. https://doi.org/10.1126/science.aad5761.

Gillett, N. P., Arora, V. K., Matthews, D., & Allen, M. R. (2013). Constraining the Ratio of Global Warming to Cumulative CO_2 Emissions Using CMIP5 Simulations. *Journal of Climate,* 26(18), 6844-6858.

Gupta, S., Tirpak, D., Burger, N., Gupta, J., Höhne, N., Boncheva, A., et al. (2007). Policies, instruments, and co-operative arrangements. In O. B. Metz, P. Bosch, R. Dave, & L. Meyer (Eds.), *Climate change 2007: mitigation. Contribution of*

Working Group III to the Fourth Assessment Report of the Intergovernmental Panel on Climate Change (pp. 745–807). Cambridge, United Kingdom and New York, NY, USA: Cambridge University Press.

Held, I. M., & Soden, B. J. Robust responses of the hydrological cycle to global warming. Journal of Climate, 2006, 19 (21), 5686-5699.

Hijioka, Y., Lin, E., Pereira, J. J., Corlett, R. T., Cui, X., Insarov, G. E., et al. (2014). Asia. In V. R. Barros, C. B. Field, D. J. Dokken, M. D. Mastrandrea, K. J. Mach, T. E. Bilir, M. Chatterjee, K. L. Ebi, Y. O. Estrada, R. C. Genova, B. Girma, E. S. Kissel, A. N. Levy, S. MacCracken, P. R. Mastrandrea, & L. L. White (Eds.), *Climate Change 2014: Impacts, Adaptation, and Vulnerability. Part B: Regional Aspects. Contribution of Working Group II to the Fifth Assessment Report of the Intergovernmental Panel on Climate Change* (pp. 1327-1370). Cambridge, United Kingdom and New York, NY, USA: Cambridge University Press.

Hirabayashi, Y., Mahendran, R., Koirala, S., Konoshima, L., Yamazaki, D., Watanabe, S., et al. (2013). Global flood risk under climate change. *Nature Climate Change,* 3, 816. http://dx.doi.org/10.1038/nclimate1911.

Hoegh-Guldberg, O., Jacob, D., Taylor, M., Bindi, M., Brown, S., Camilloni, I., et al. (2018). Impacts of 1.5°C global warming on natural and human systems. In V. Masson-Delmotte, P. Zhai, H. O. Pörtner, D. Roberts, J. Skea, P. R. Shukla, A. Pirani, W. Moufouma-Okia, C. Péan, R. Pidcock, S. Connors, J. B. R. Matthews, Y. Chen, X. Zhou, M. I. Gomis, E. Lonnoy, T. Maycock, M. Tignor, & T. Waterfield (Eds.), *Global warming of 1.5°C. An IPCC Special Report on the impacts of global warming of 1.5°C above pre-industrial levels and related global greenhouse gas emission pathways, in the context of strengthening the global response to the threat of climate change, sustainable development, and efforts to eradicate poverty*: In Press.

IPCC. (2014). *Climate Change 2014: Synthesis Report. Contribution of Working Groups I, II and III to the Fifth Assessment Report of the Intergovernmental Panel on Climate Change*. Cambridge, UK, and New York, NY, USA: Cambridge University Press.

Jones, B., & O'Neill, B. C. (2016). Spatially explicit global population scenarios consistent with the Shared Socioeconomic Pathways. *Environmental Research Letters,* 11(8), 084003. http://stacks.iop.org/1748-9326/11/i=8/a=084003.

Karmalkar, A. V., & Bradley, R. S. (2017). Consequences of Global Warming of 1.5°C and 2.0°C for Regional Temperature and Precipitation Changes in the Contiguous United States. *PLOS ONE,* 12(1), e0168697. https://doi.org/10.1371/journal.pone.0168697.

Kharin, V. V., Flato, G. M., Zhang, X., Gillett, N. P., Zwiers, F., & Anderson, K. J. (2018). Risks from Climate Extremes Change Differently from 1.5°C to 2.0°C Depending on Rarity. *Earth's Future,* 6(5), 704-715. https://doi.org/10.1002/2018EF000813.

Kharin, V. V., & Zwiers, F. W. (2005). Estimating Extremes in Transient Climate Change Simulations. *Journal of Climate,* 18(18), 1156-1173.

King, A. D., Donat, M. G., Lewis, S. C., Henley, B. J., Mitchell, D. M., Stott, P. A., et al.

(2018). Reduced heat exposure by limiting global warming to 1.5°C. *Nature Climate Change,* 8(7), 549-551.

King, A. D., Karoly, D. J., & Henley, B. J. (2017). Australian climate extremes at 1.5 °C and 2 °C of global warming. *Nature Climate Change,* 7(6), 412-416.

Lavell, A., Oppenheimer, M., Diop, C., Hess, J., Lempert, R., Li, J., et al. (2012). Climate change: new dimensions in disaster risk, exposure, vulnerability, and resilience. In C. B. Field, V. Barros, T. F. Stocker, D. Qin, D. J. Dokken, K. L. Ebi, M. D. Mastrandrea, K. J. Mach, G.-K. Plattner, S. K. Allen, M. Tignor, & P. M. Midgley (Eds.), *Managing the Risks of Extreme Events and Disasters to Advance Climate Change Adaptation. A Special Report of Working Groups I and II of the Intergovernmental Panel on Climate Change (IPCC)* (pp. 25-64). Cambridge, UK, and New York, NY, USA: Cambridge University Press.

Li, D., Zhou, T., Zou, L., Zhang, W., & Zhang, L. (2018). Extreme High-Temperature Events Over East Asia in 1.5°C and 2.0°C Warmer Futures: Analysis of NCAR CESM Low-Warming Experiments. *Geophysical Research Letters,* 45(3), 1541-1550.

Matthews, H. D., Gillett, N. P., Stott, P. A., & Zickfeld, K. (2009). The proportionality of global warming to cumulative carbon emissions. *Nature,* 459, 829. https://doi.org/10.1038/nature08047.

Mueller, B., & Seneviratne, S. I. (2012). Hot days induced by precipitation deficits at the global scale. *Proceedings of the National Academy of Sciences,* 109(31), 12398. http://www.pnas.org/content/109/31/12398.abstract.

Orlowsky, B., & Seneviratne, S. I. (2012). Global changes in extreme events: regional and seasonal dimension. *Climatic Change,* 110(3), 669-696. journal article. https://doi.org/10.1007/s10584-011-0122-9.

Prudhomme, C., Giuntoli, I., Robinson, E. L., Clark, D. B., Arnell, N. W., Dankers, R., et al. (2014). Hydrological droughts in the 21st century, hotspots and uncertainties from a global multimodel ensemble experiment. *Proceedings of the National Academy of Sciences,* 111(9), 3262-3267. http://www.pnas.org/content/pnas/111/9/3262.full.pdf.

Rogelj, J., den Elzen, M., Höhne, N., Fransen, T., Fekete, H., Winkler, H., et al. (2016). Paris Agreement climate proposals need a boost to keep warming well below 2 °C. *Nature,* 534, 631. Perspective. https://doi.org/10.1038/nature18307.

Sanderson, B. M., O'Neill, B. C., & Tebaldi, C. (2016). What would it take to achieve the Paris temperature targets? *Geophysical Research Letters,* 43(13), 7133-7142. https://doi.org/10.1002/2016GL069563.

Sanderson, B. M., Xu, Y., Tebaldi, C., Wehner, M., O'Neill, B., Jahn, A., et al. (2017). Community climate simulations to assess avoided impacts in 1.5 and 2 °C futures. *Earth Syst. Dynam.,* 8(3), 827-847. https://www.earth-syst-dynam.net/8/827/2017/.

Schleussner, C.-F., Lissner, T. K., Fischer, E. M., Wohland, J., Perrette, M., Golly, A., et al. (2016). Differential climate impacts for policy-relevant limits to global warming: the case of 1.5 °C and 2 °C. *Earth System Dynamics,* 7(2), 327-351.

Sebastian, D. E., Pathak, A., & Ghosh, S. (2016). Use of Atmospheric Budget to Reduce Uncertainty in Estimated Water Availability over South Asia from Different Reanalyses. *Scientific Reports,* 6, 29664. Article. http://dx.doi.org/10.1038/srep29664.

Seneviratne, S. I., Nicholls, N., Easterling, D., Goodess, C. M., Kanae, S., Kossin, J., et al. (2012). Changes in climate extremes and their impacts on the natural physical environment. In C. B. Field, V. Barros, T. F. Stocker, D. Qin, D. J. Dokken, K. L. Ebi, M. D. Mastrandrea, K. J. Mach, G.-K. Plattner, S. K. Allen, M. Tignor, & P. M. Midgley (Eds.), *Managing the Risks of Extreme Events and Disasters to Advance Climate Change Adaptation. A Special Report of Working Groups I and II of the Intergovernmental Panel on Climate Change* (pp. 109-230). Cambridge, UK, and New York, NY, USA: Cambridge University Press.

Seneviratne, S. I., Rogelj, J., Séférian, R., Wartenburger, R., Allen, M. R., Cain, M., et al. (2018). The many possible climates from the Paris Agreement's aim of 1.5°C warming. *Nature,* 558(7708), 41-49. https://doi.org/10.1038/s41586-018-0181-4.

Shi, C., Jiang, Z.-H., Chen, W.-L., & Li, L. (2018). Changes in temperature extremes over China under 1.5°C and 2.0°C global warming targets. *Advances in Climate Change Research,* 9(2), 120-129. http://www.sciencedirect.com/science/article/pii/S167492781730103X.

Taylor, K. E., Stouffer, R. J., & Meehl, G. A. (2011). An Overview of CMIP5 and the Experiment Design. *Bulletin of the American Meteorological Society,* 93(4), 485-498. https://doi.org/10.1175/BAMS-D-11-00094.1.

Tokarska, K. B., Gillett, N. P., Weaver, A. J., Arora, V. K., & Eby, M. (2016). The climate response to five trillion tonnes of carbon. *Nature Climate Change, 6*(9), 851-855. https://www.nature.com/articles/nclimate3036.

UNEP. (2017). *The Emissions Gap Report*. Retrieved from Nairobi.

UNFCCC. (2015a). *Adoption of the Paris Agreement: Proposal by the President*. Geneva.

UNFCCC. (2015b). *Synthesis report on the aggregate effect of the intended nationally determined contributions*. Paris.

UNFCCC. (2018). National Inventory Submissions. http://unfccc.int/national_reports/annex_i_ghg_inventories/national_inventories_submissions/items/10566.php.

Wang, F., Ge, Q., Chen, D., Luterbacher, J., Tokarska, K. B., & Hao, Z. (2018). Global and regional climate responses to national-committed emission reductions under the Paris agreement. *Geografiska Annaler: Series A, Physical Geography,* 100(3), 240-253. https://doi.org/10.1080/04353676.2018.1488538.

Xu, Y., Zhou, B.-T., Wu, J., Han, Z.-Y., Zhang, Y.-X., & Wu, J. (2017). Asian climate change under 1.5–4 °C warming targets. *Advances in Climate Change Research,* 8(2), 99-107. http://www.sciencedirect.com/science/article/pii/S1674927817300333.

Zhang, W., Zhou, T., Zou, L., Zhang, L., & Chen, X. (2018). Reduced exposure to extreme precipitation from 0.5 °C less warming in global land monsoon regions. *Nature Communications,* 9(1), 3153.

https://doi.org/10.1038/s41467-018-05633-3.

Zhang, X., Alexander, L., Hegerl, G. C., Jones, P., Tank, A. K., Peterson, T. C., et al. (2011). Indices for monitoring changes in extremes based on daily temperature and precipitation data. *Wiley Interdisciplinary Reviews: Climate Change,* 2(6), 851-870. https://onlinelibrary.wiley.com/doi/abs/10.1002/wcc.147.

Zhou T, Ren L, and Liu H, et al. Impact of 1.5°C and 2.0°C global warming on aircraft takeoff performance in China. Sci. Bull. 2018; 63: 700–707.

Zickfeld, K., Eby, M., Matthews, H. D., & Weaver, A. J. (2009). Setting cumulative emissions targets to reduce the risk of dangerous climate change. *Proceedings of the National Academy of Sciences,* 106(38), 16129-16134. http://www.pnas.org/content/pnas/106/38/16129.full.pdf.

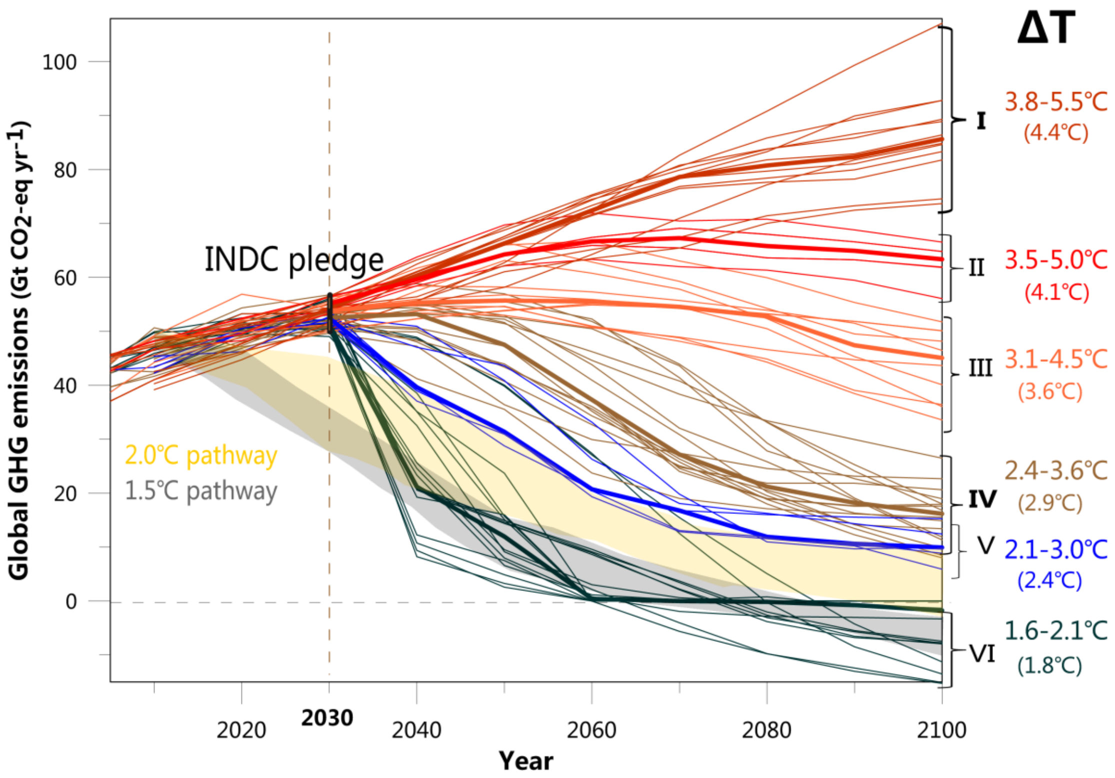

Figure 1. Future emission pathways analyzed in this study. The black vertical line represents the range of conditional and unconditional INDC pledges in 2030; thin lines in different colors show the selected emission pathways clustered into the six groups. The range of the 1.5°C and 2.0°C pathways are plotted for reference, in grey and orange shaded areas, respectively (CAT, 2017). The estimates of warming at the end of the 21st century above the pre-industrial level (ΔT) for each scenario group are labelled on the right (uncertainty range of 33-66% and median in brackets).

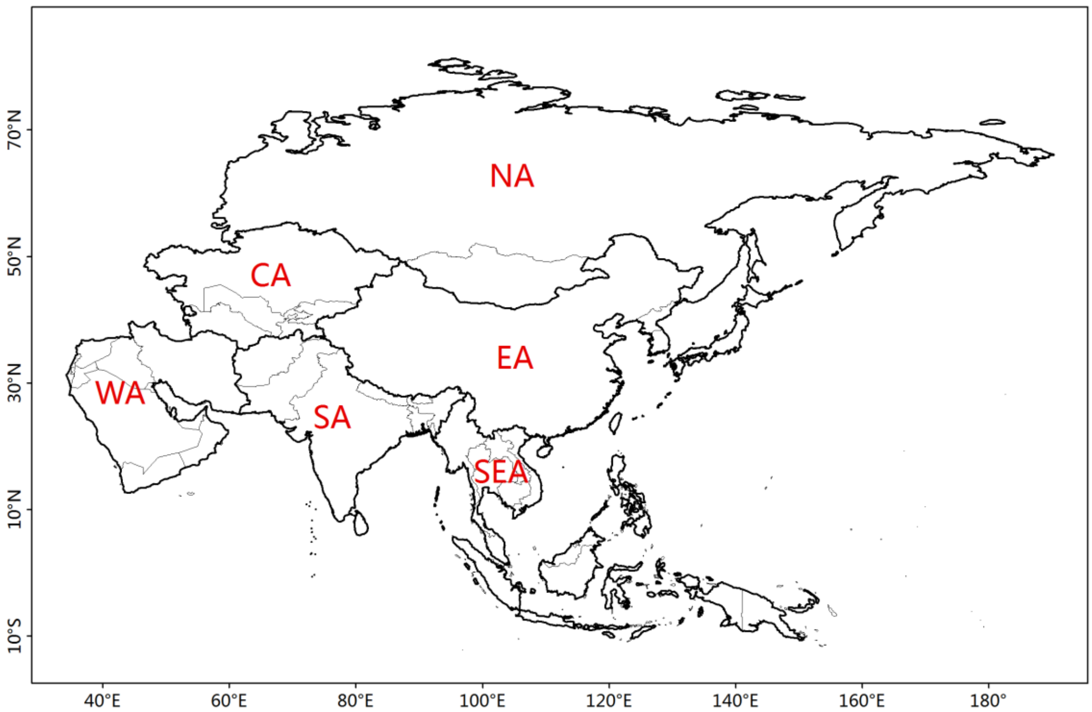

Figure 2 Sub-regions in Asia.

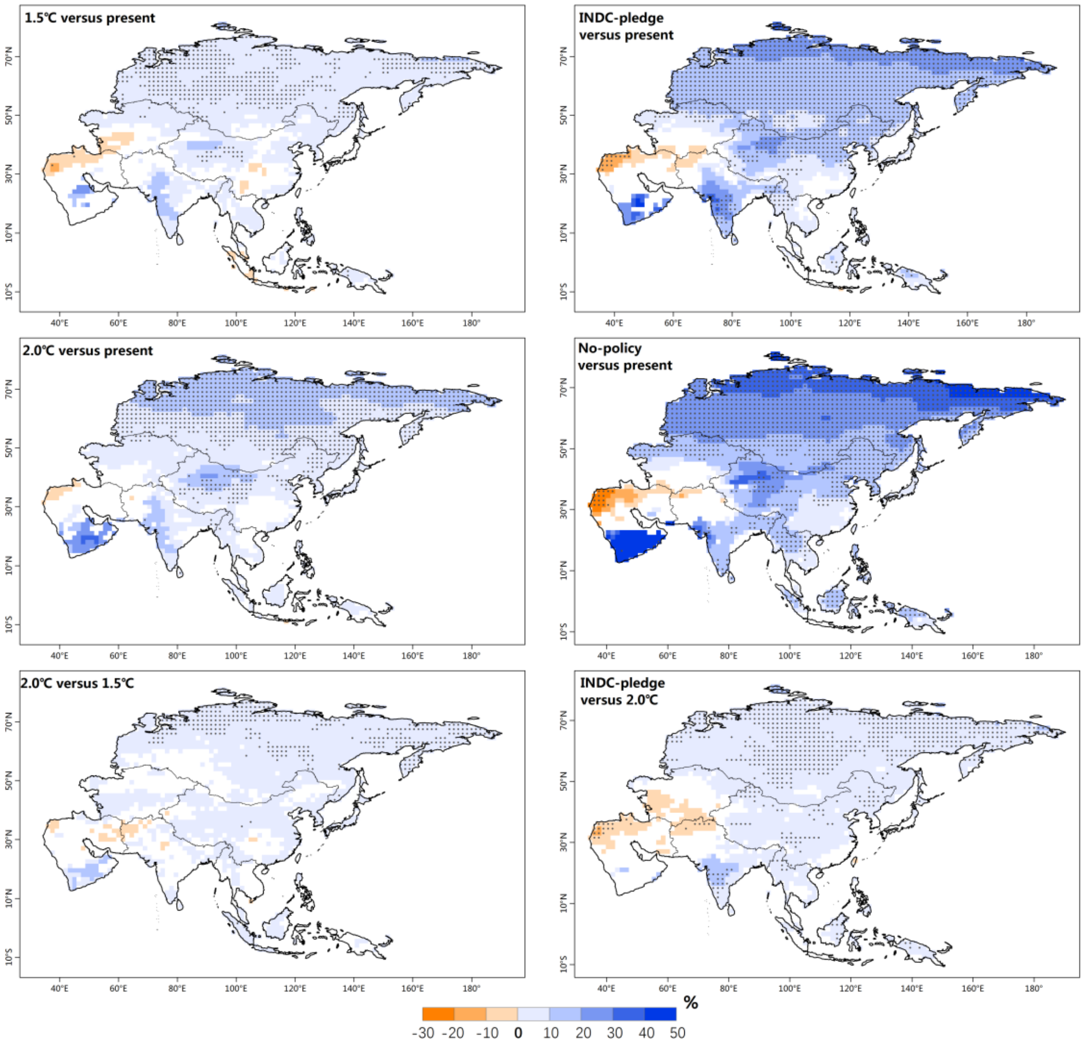

Figure 3. **Relative changes in annual mean precipitation over Asia, based on multi-model median.** Colored shading is applied for areas where at least 66% of the models agree on the sign of the change; black stippling indicates regions where at least 90% of all models agree on the sign of the change.

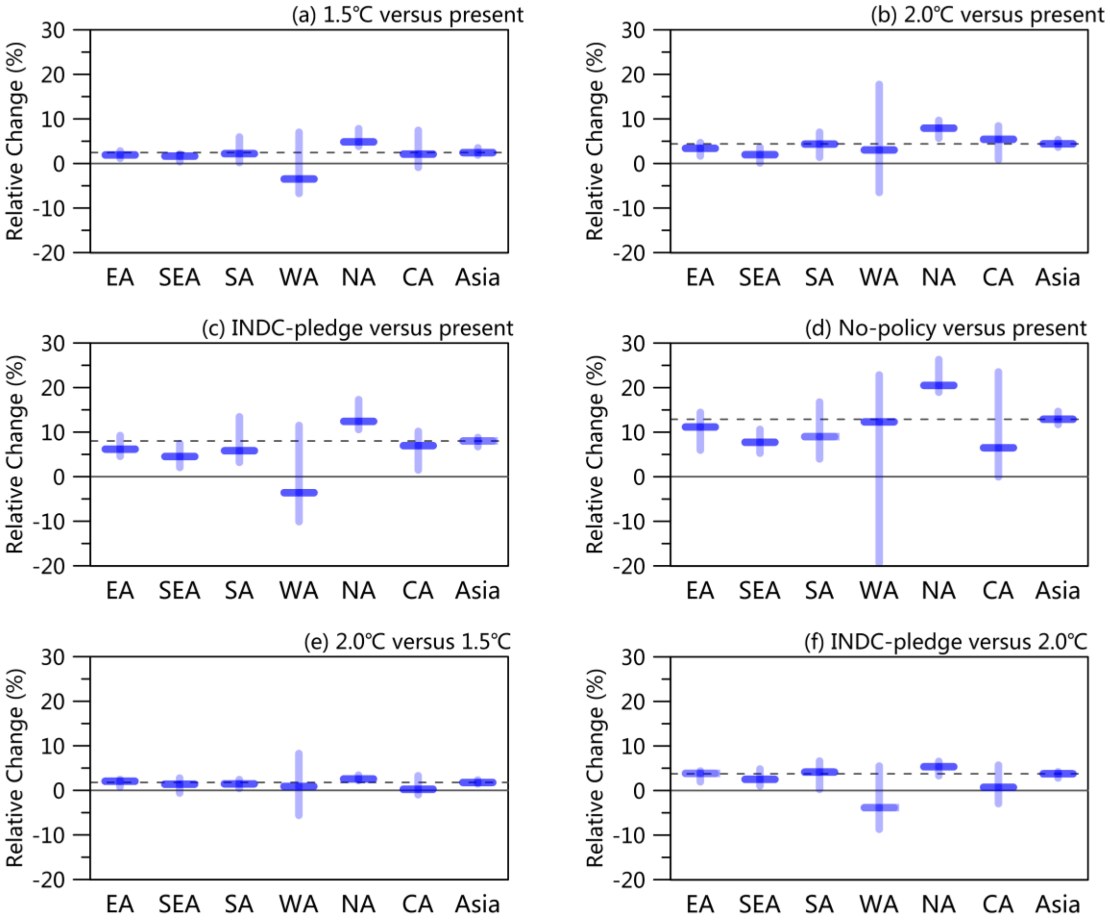

Figure 4. Regional average differences among different scenarios in the annual mean precipitation changes in Asia and the six sub-regions. Central lines and bars in blue denote multimodal medians and interquartile ranges, respectively. Horizontal dashed and solid lines in grey indicate the value of Asian mean and zero, respectively.

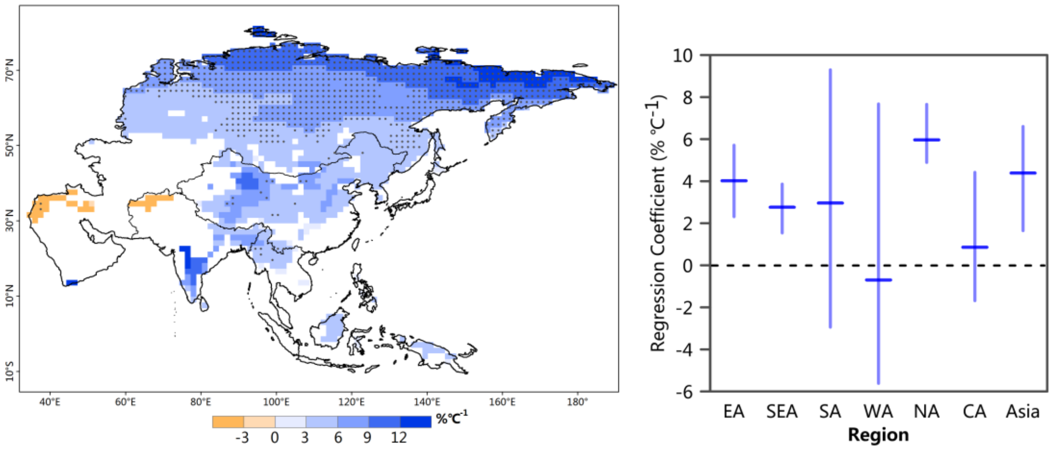

Figure 5. **Annual mean precipitation response to global temperature increase, per degree of warming.** Regression coefficients are calculated in each grid cell based on the local precipitation and global mean temperature of seperate models, and then estimated the multimodel ensemble median. **Left**: Spatial distribution of multimodel median: colored shading is applied for areas where at least 66% of the models agree on the significant of linear relationship (statistically significant at the 5% level based on the Student's t-test); black stippling indicates regions where at least 90% of all models agree on the significant of linear relationship.. **Right**: Regional average: Central lines and bars show the multimodel ensemble 25th, 50th, and 75th intervals.

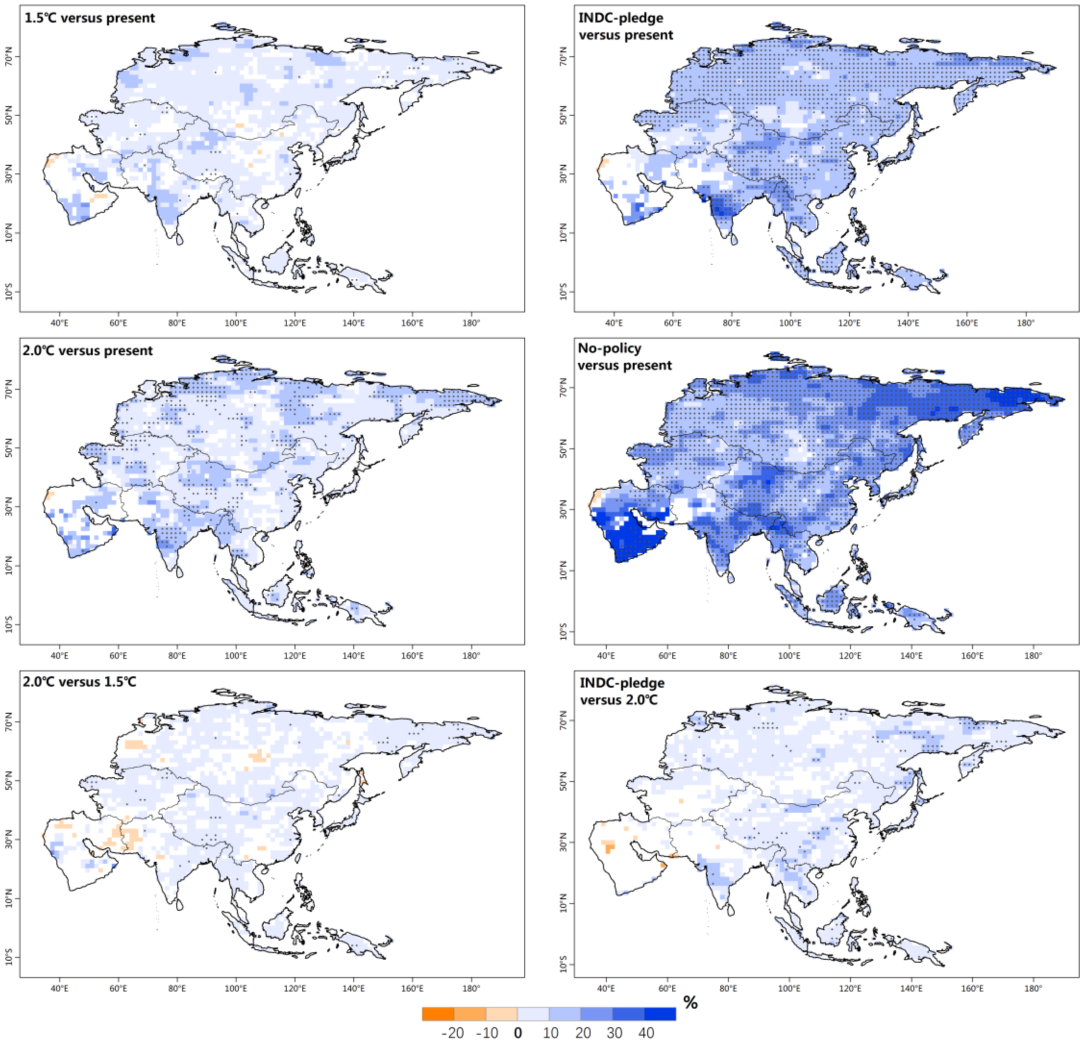

Figure 6. Relative changes in the annual Rx5day over Asia, based on the multi-model median. Increased dryness is indicated with yellow to orange colors; decreased dryness with blue. Colored shading is applied to areas where at least 66% of the models agree on the sign of the change; stippling is added for regions where at least 90% of all models agree on the sign of the change.

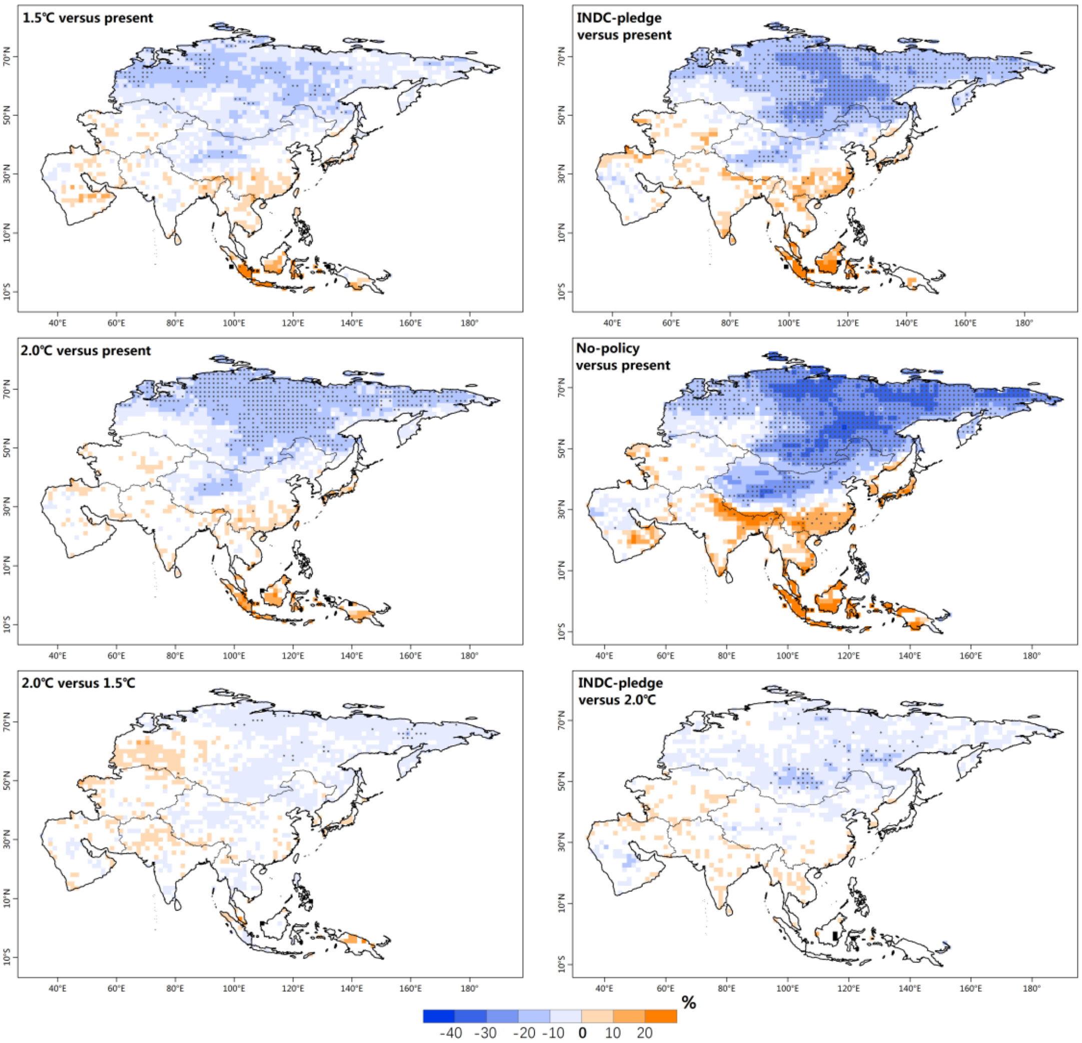

Figure 7. **Relative changes in annual CDD over Asia, based on the multi-model median.**

Corresponds to Fig. 6, but for CDD.

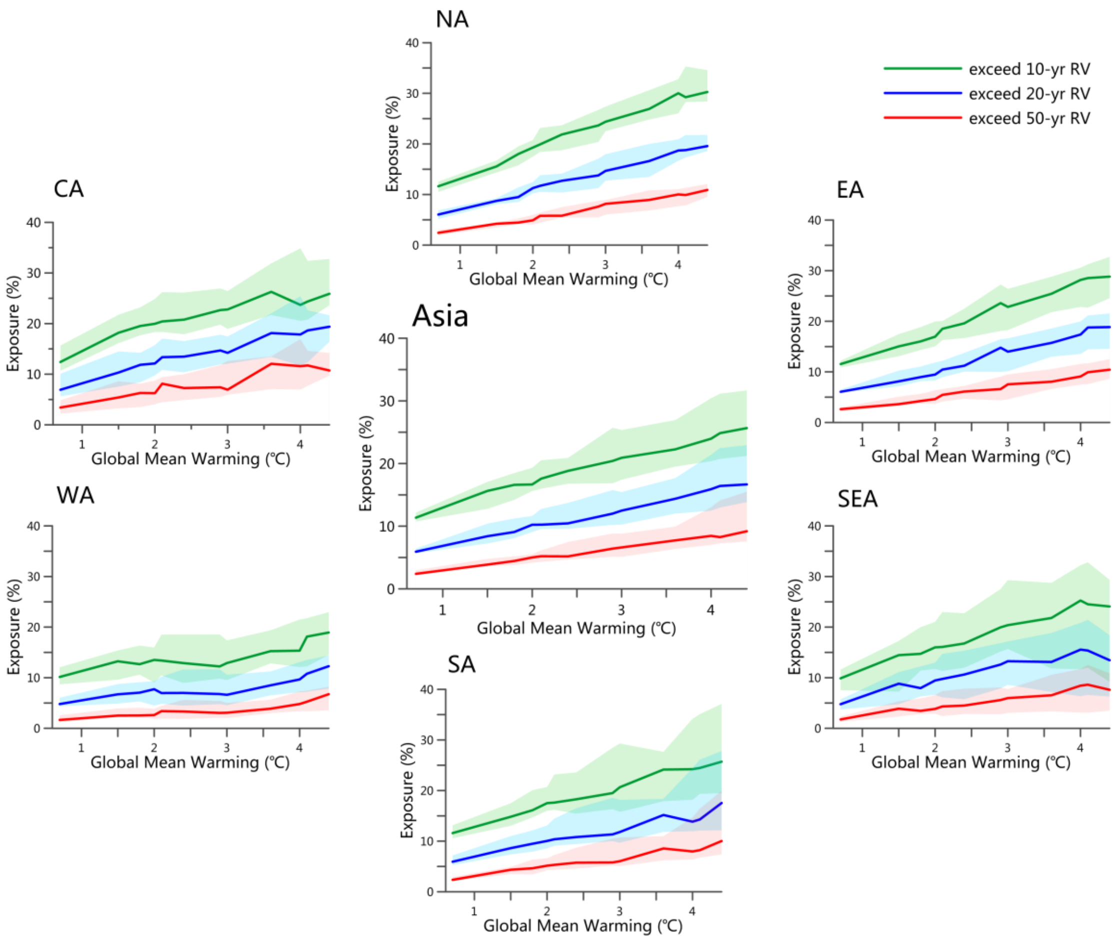

Figure 8. **Population exposure to heavy rainfall events of different RVs.** The population density weighted means for Asia and the six sub-regions are estimated based on the year-2100 population projection under the SSP2 scenario (for future scenarios) and the year 2000 baseline (for present day). The multimodel medians are in solid lines, and interquartile ranges are shaded. Results of areal exposure refer to Fig. S4.

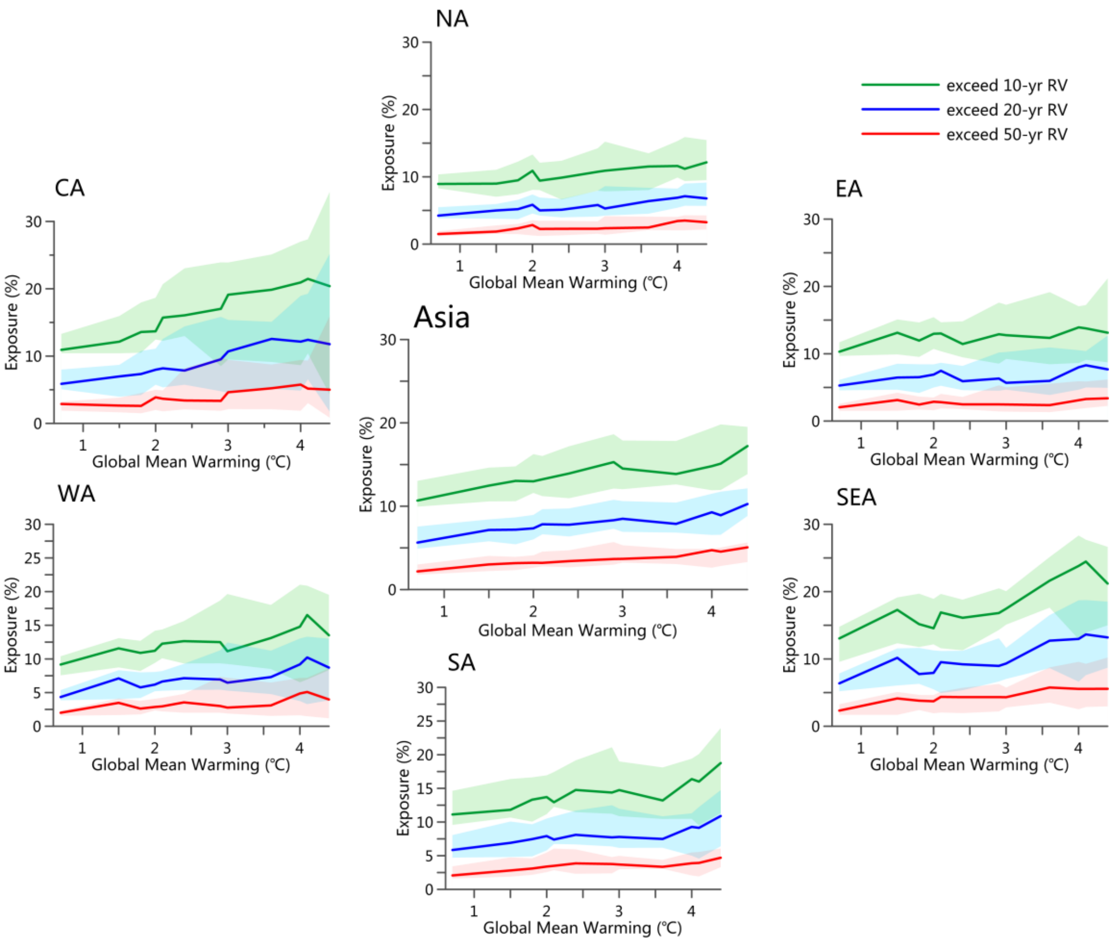

Figure 9. **Population exposure to dry spell events of different RVs.** Corresponds to Fig. 8, but for population exposure to dry spell events. Results of areal exposure refer to Fig. S5.

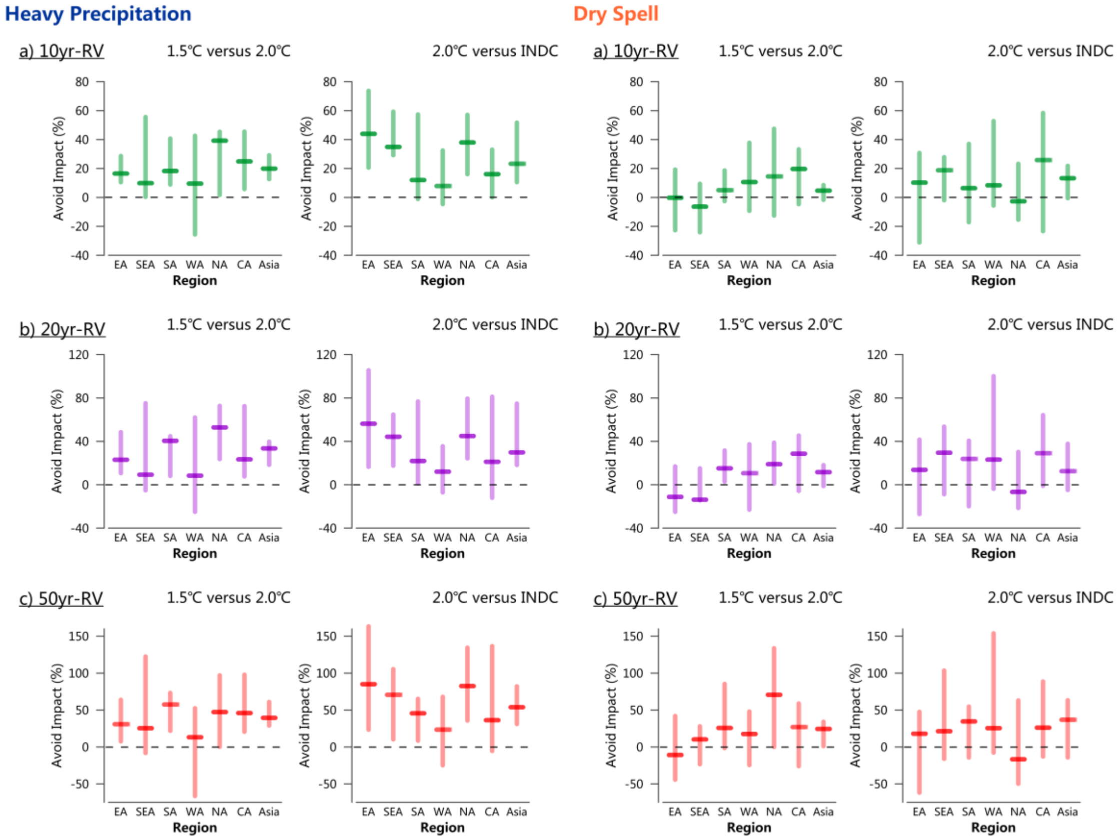

Figure 10. Changes in extreme heavy rainfall (two left panels) and dry spell events (two right panels) avoided over Asia and its sub-regions in less warming scenarios. Population exposure is reduced in the low warming scenarios (1.5°C compared to 2.0°C, 2.0°C compare to INDC-pledge) for heavy rainfall (columns 1 and 2) and dry spell (columns 3 and 4) events that exceed the baseline (a) 10-, (b) 20- and (c) 50-year return values. Central lines and bars denote multimodal medians and interquartile ranges, respectively. Results based on areal exposure refer to Fig. S6.